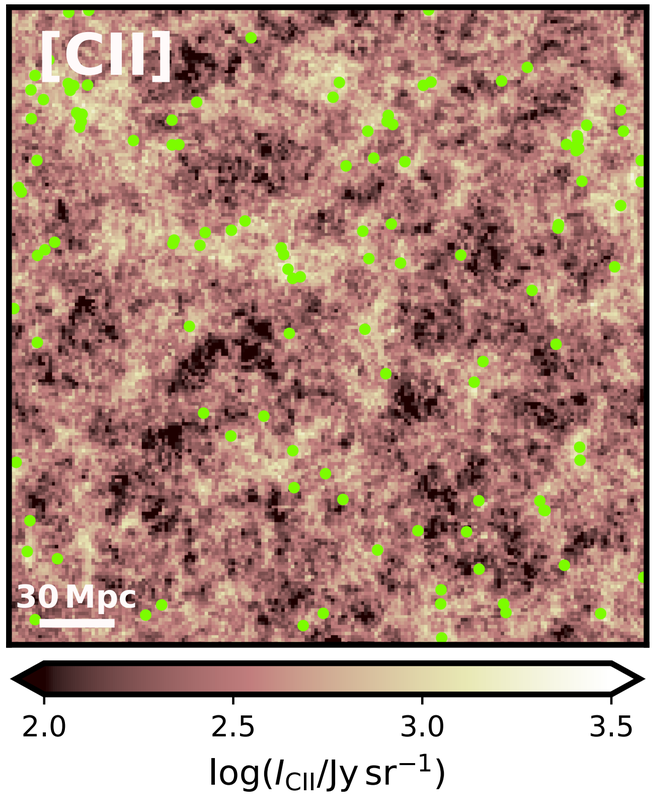

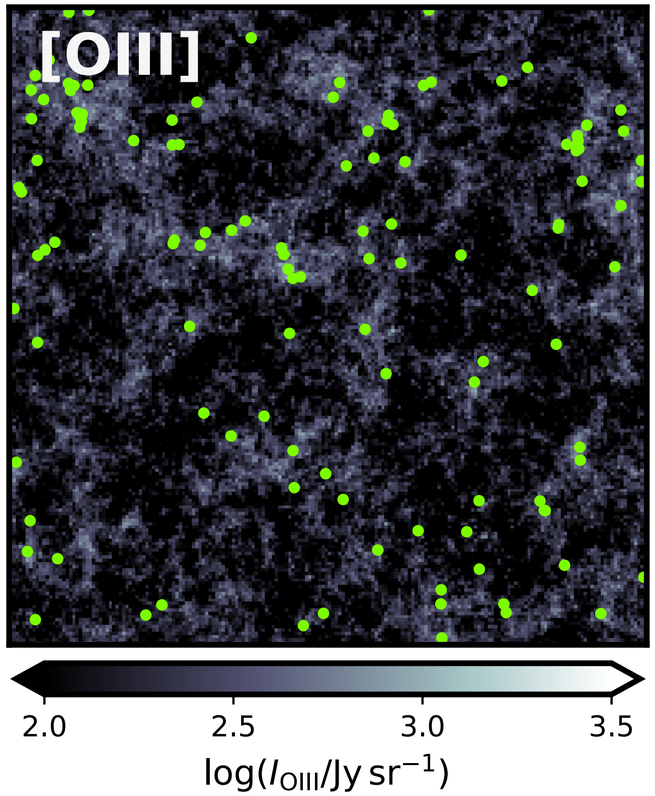

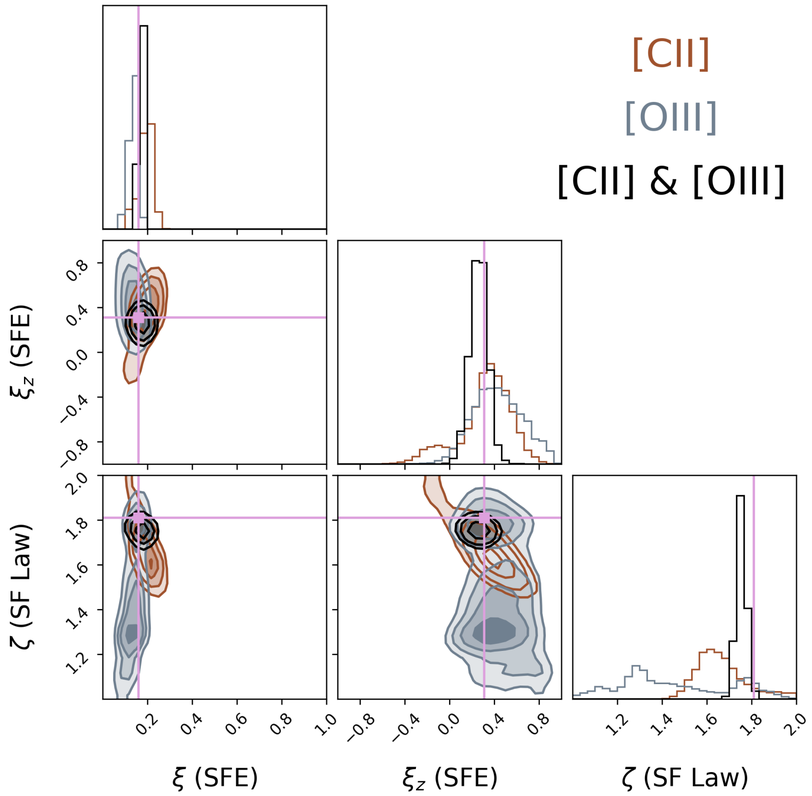

Harnessing the power of mm-wave intensity mapping to study early galaxy formation

Guochao (Jason) Sun | CIERA Fellow at Northwestern University

Collaborators: T. Nguyen, T. Starkenburg, **B. Scott**, C.-A. Faucher-Giguère (NU/CIERA/SkAI)
A. Lidz (Penn), T.-C. Chang (JPL/Caltech), S. Furlanetto (UCLA)

Line Intensity Mapping 2025 | Annecy, France 🇫🇷 | June 4, 2025

Funded by the U.S. National Science Foundation and the Simons Foundation

High-redshift Universe: fascinating by its many unknowns

- When and how did first galaxies form?
- What drove cosmic reionization and how?
- What were first black holes like?
- Unique lab for new physics?

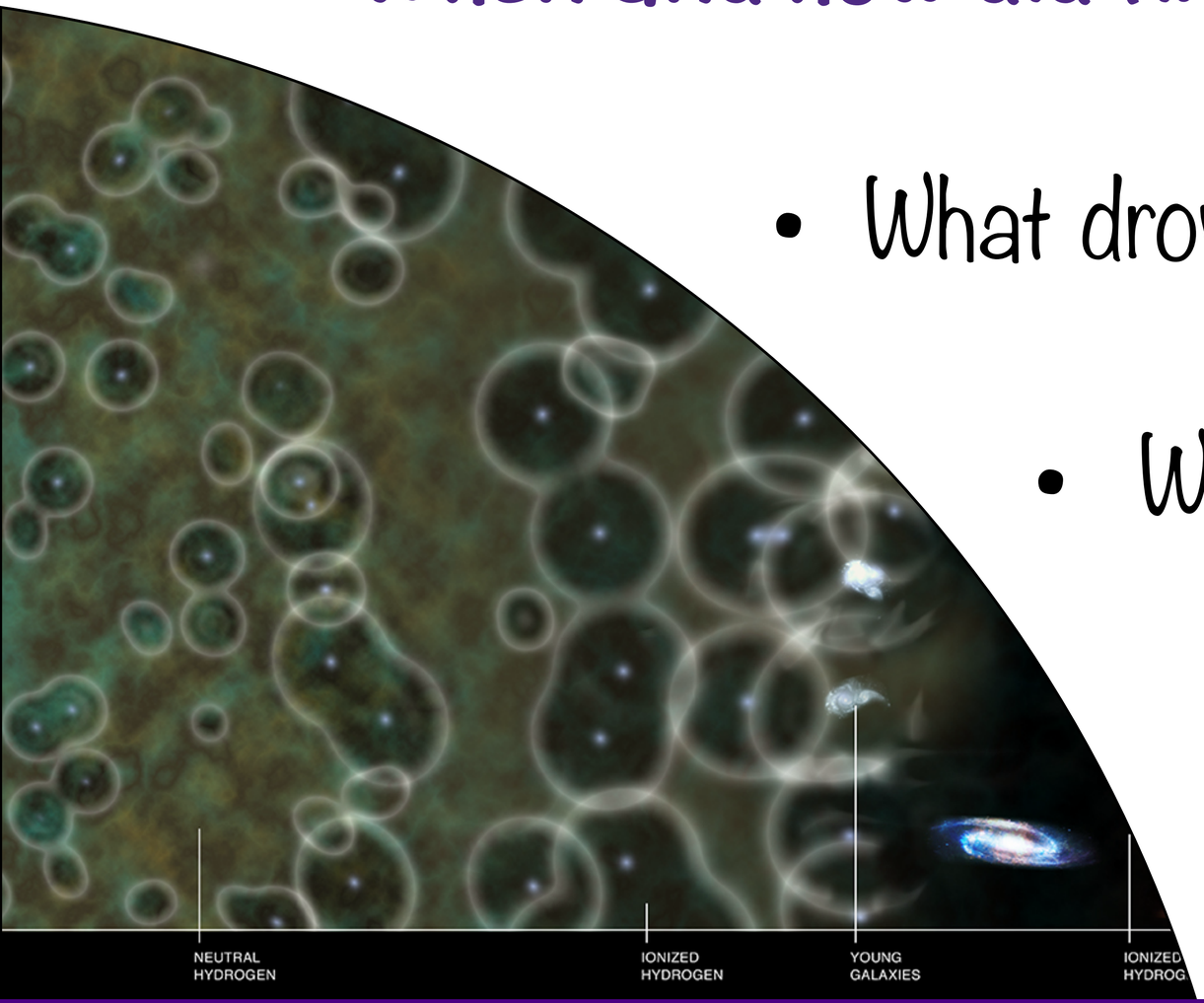

Star formation efficiency (stellar mass-halo mass relation)

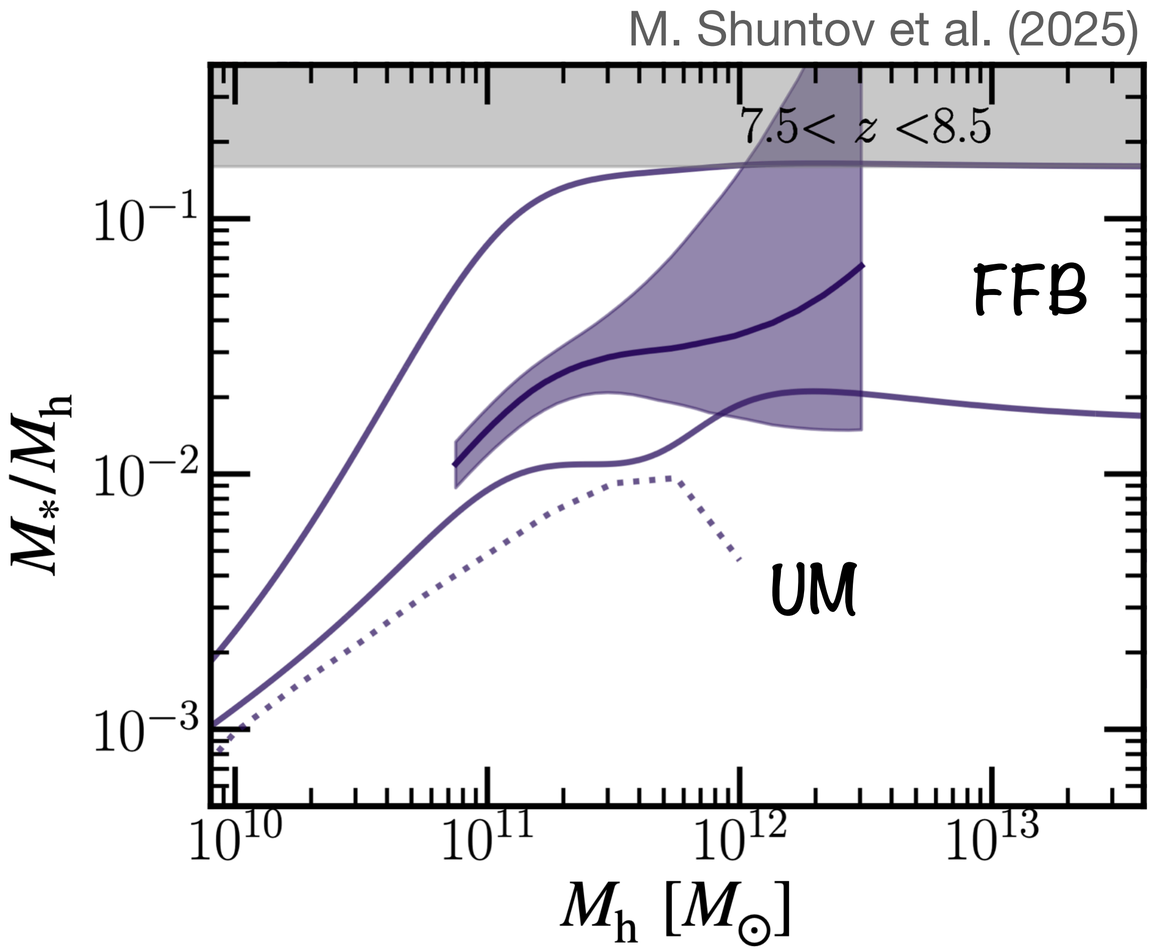

- **Probe of stellar feedback**
- **Mass & redshift dependence**

Star formation law (a.k.a. Kennicutt-Schmidt relation)

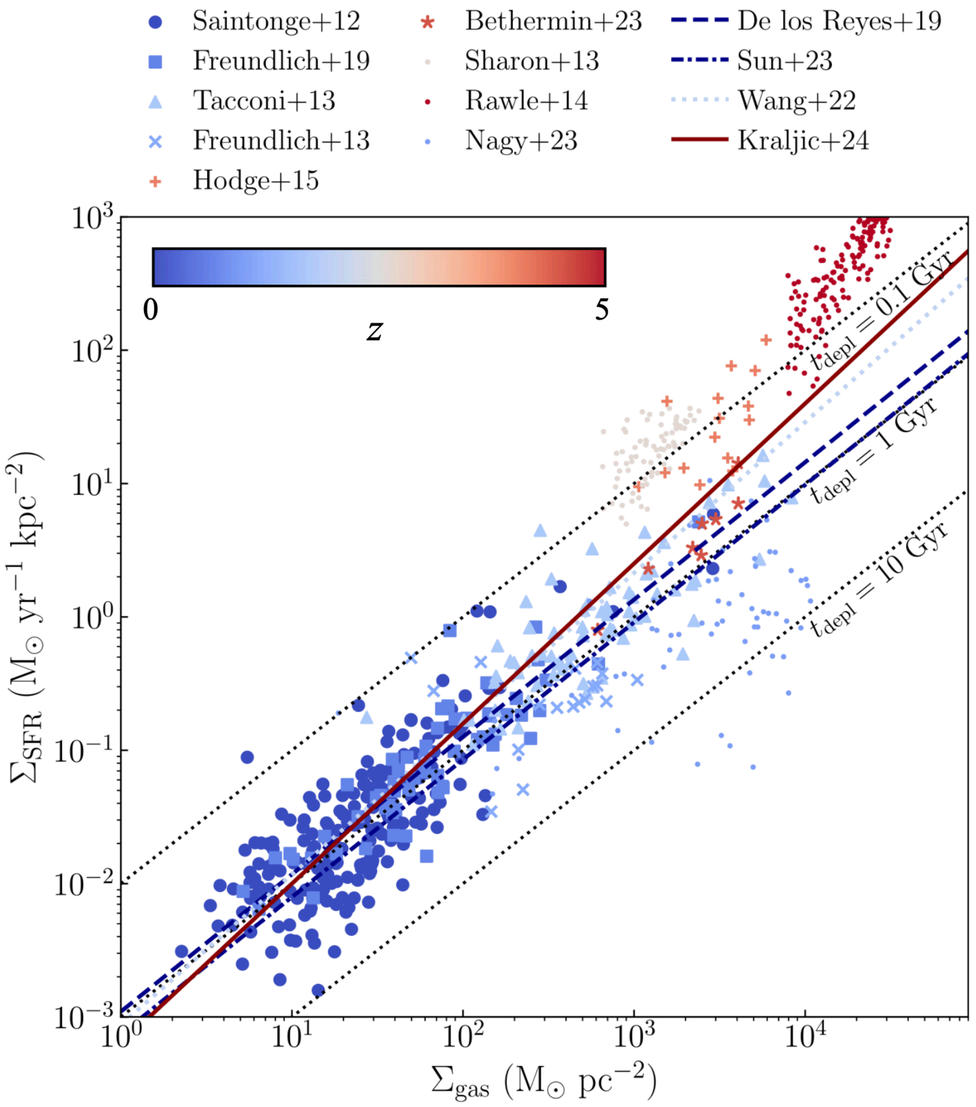

J. Freundlich et al. (2024)

- **Surface densities & gas depletion time**
- **Slope: denser gas better at SF (if > 1)**

LIMFAST: 21cmFAST extension for multi-tracer IM

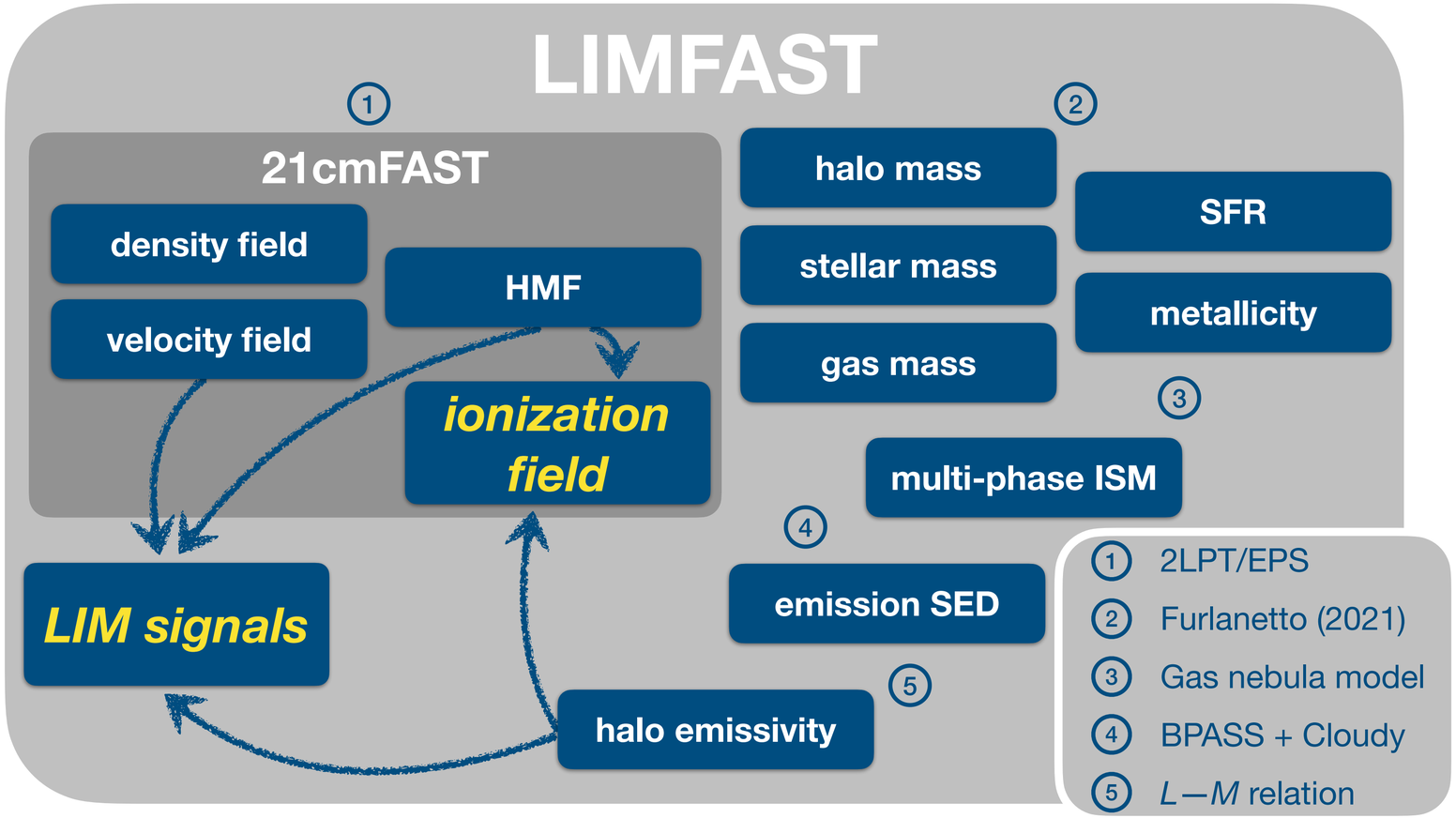

- L. Mas-Ribas, **GS** et al. (2023): Methodology & LIM predictions
- **GS** et al. (2023): LIM for high-z galaxy formation
- **GS** et al. (2025): 21cm^2—NIRB cross-correlation
- **GS et al. (2025, in prep.): Parameter inference from LIM**

Gas-regulator model for feedback-regulated star formation

Mass loading factor

$$\eta(M_{\rm h}, z) = \eta_0 \left(\frac{M_{\rm h}}{10^{11.5}\, M_\odot} \right)^{-\xi} \left(\frac{1+z}{9} \right)^{-\xi_z}$$

Star formation law

$$\dot{\Sigma}_\star(\Sigma_{\rm g}, z) = \epsilon_{\star,0} \frac{\Sigma_{\rm g,0}}{t_{\rm ff,0}^{\rm disc}} \left(\frac{\Sigma_{\rm g}}{\Sigma_{\rm g,0}} \right)^{\zeta} \left(\frac{1+z}{9} \right)^{\zeta_z}$$

- ξ — $M_{\rm h}$ dependence of mass loading factor
- ξ_z — z dependence of mass loading factor
- ζ — slope of star formation law

Halo mass

$$\frac{\tilde{M}'_{\rm h}}{\tilde{M}_{\rm h}} = -\mathscr{M}_0$$

Gas mass

$$\frac{\tilde{M}'_{\rm g}}{\tilde{M}_{\rm g}} = \mathscr{M}_0 \left[-\frac{1}{X_{\rm g}} + \eta_0 \dot{X}_{\star,0} \left(\frac{X_{\rm g}}{X_{\rm g,0}} \right)^{\alpha_X} \tilde{M}_{\rm h}^{\alpha_m} \left(\frac{1+z}{1+z_0} \right)^{\alpha_z} \right]$$

Stellar mass

$$\tilde{M}'_\star = -\mathscr{M}_0 \dot{X}_{\star,0} \left(\frac{X_{\rm g}}{X_{\rm g,0}} \right)^{\beta_X} \tilde{M}_{\rm h}^{\beta_m} \left(\frac{1+z}{1+z_0} \right)^{\beta_z}$$

Gas retention

$$\frac{X'_{\rm g}}{X_{\rm g}} = \frac{\tilde{M}'_{\rm g}}{\tilde{M}_{\rm g}} - \frac{\tilde{M}'_{\rm h}}{\tilde{M}_{\rm h}}$$

Metal mass

$$\tilde{M}'_Z = \left[y_Z - \eta \left(\tilde{M}_Z / \tilde{M}_{\rm g} \right) \right] \tilde{M}'_\star$$

GS et al. (2025, in prep.; see also S. Furlanetto 21)

Halo properties respond differently to SFE & SF law

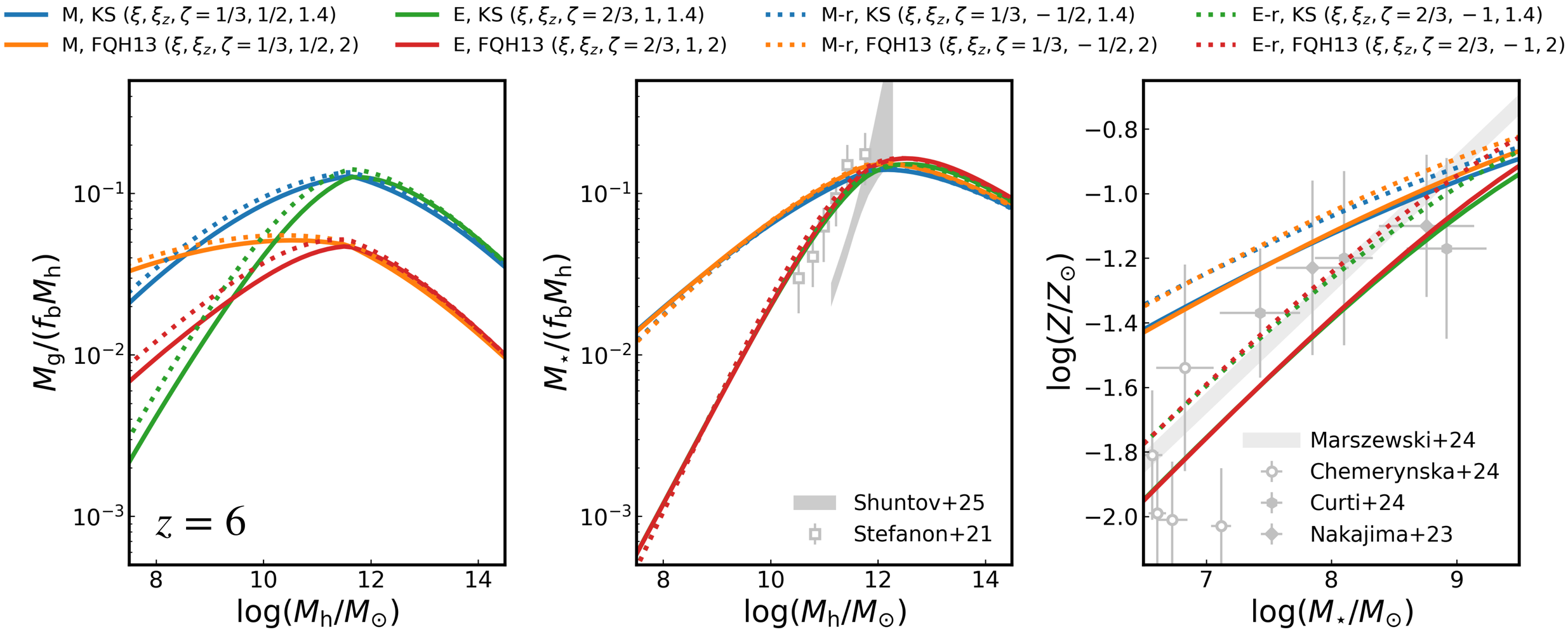

GS et al. (2025, in prep.)

Multi-line emission: a toy model of multi-phase gas nebula

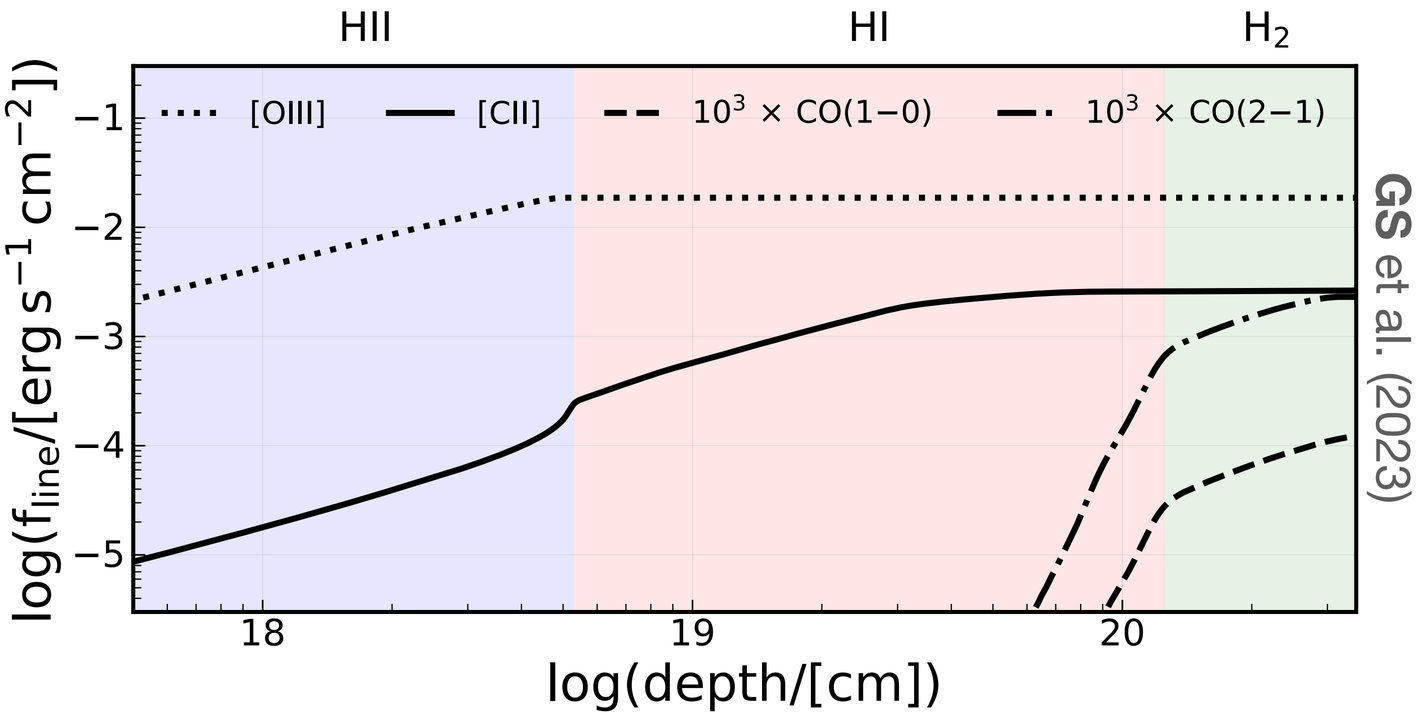

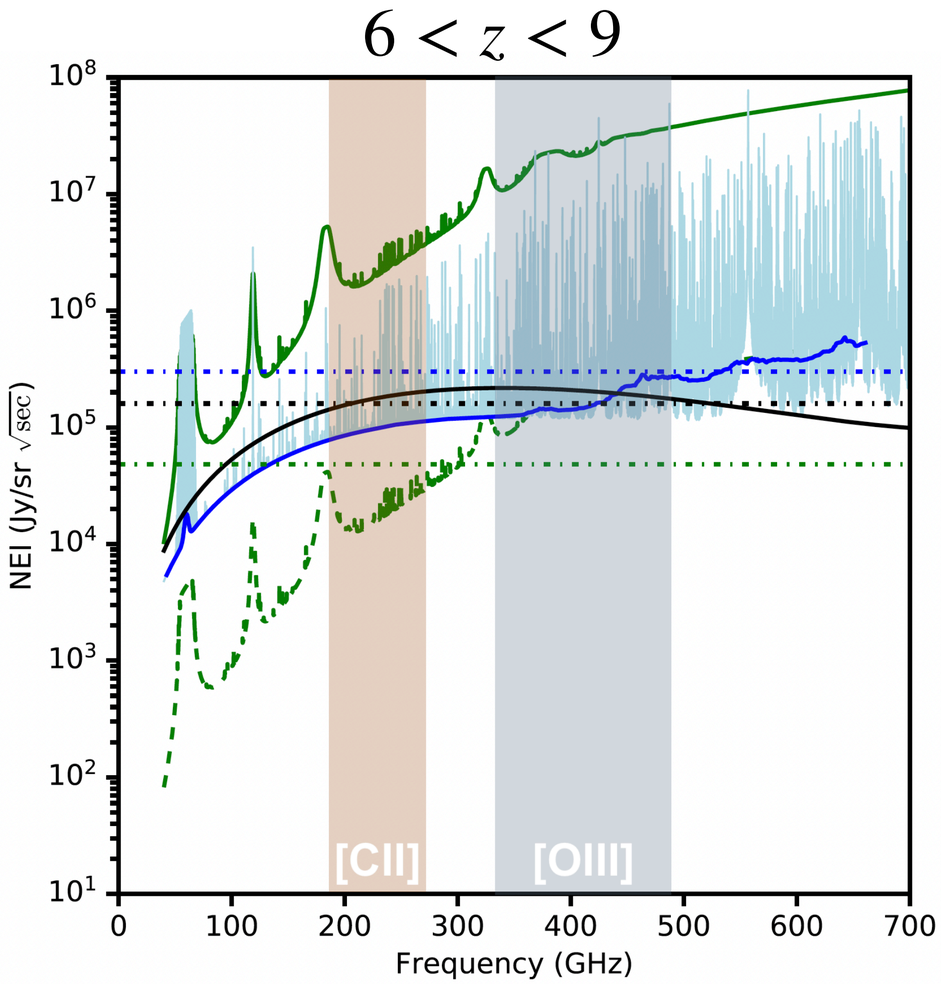

- **CLOUDY-based line emissivities**
- **Convolved w/ turbulent GMC density PDF**
- **Scaled by halo stellar/gas mass content**

H. Padmanabhan et al. (2022)

$L_{[CII]}$ & $L_{[OIII]}$ under varying SFE & SF law assumptions

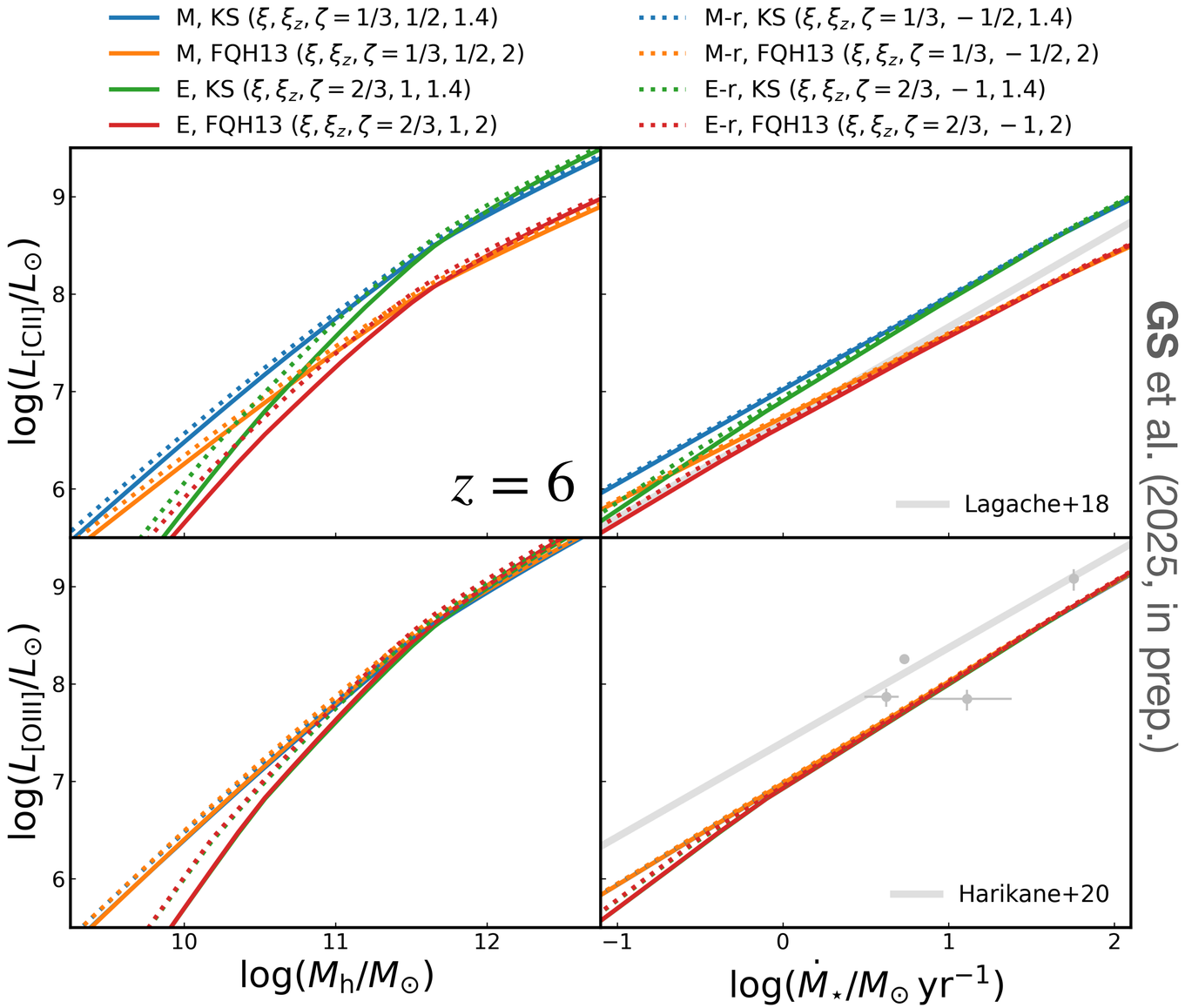

- **[CII] affected by both SFE & SF law**
- **[OIII] affected ~solely by SFE**

Simulating [CII], [OIII], and their cross-correlation w/ LBGs

Roman LBGs with $m_{\rm AB} < -27.2$

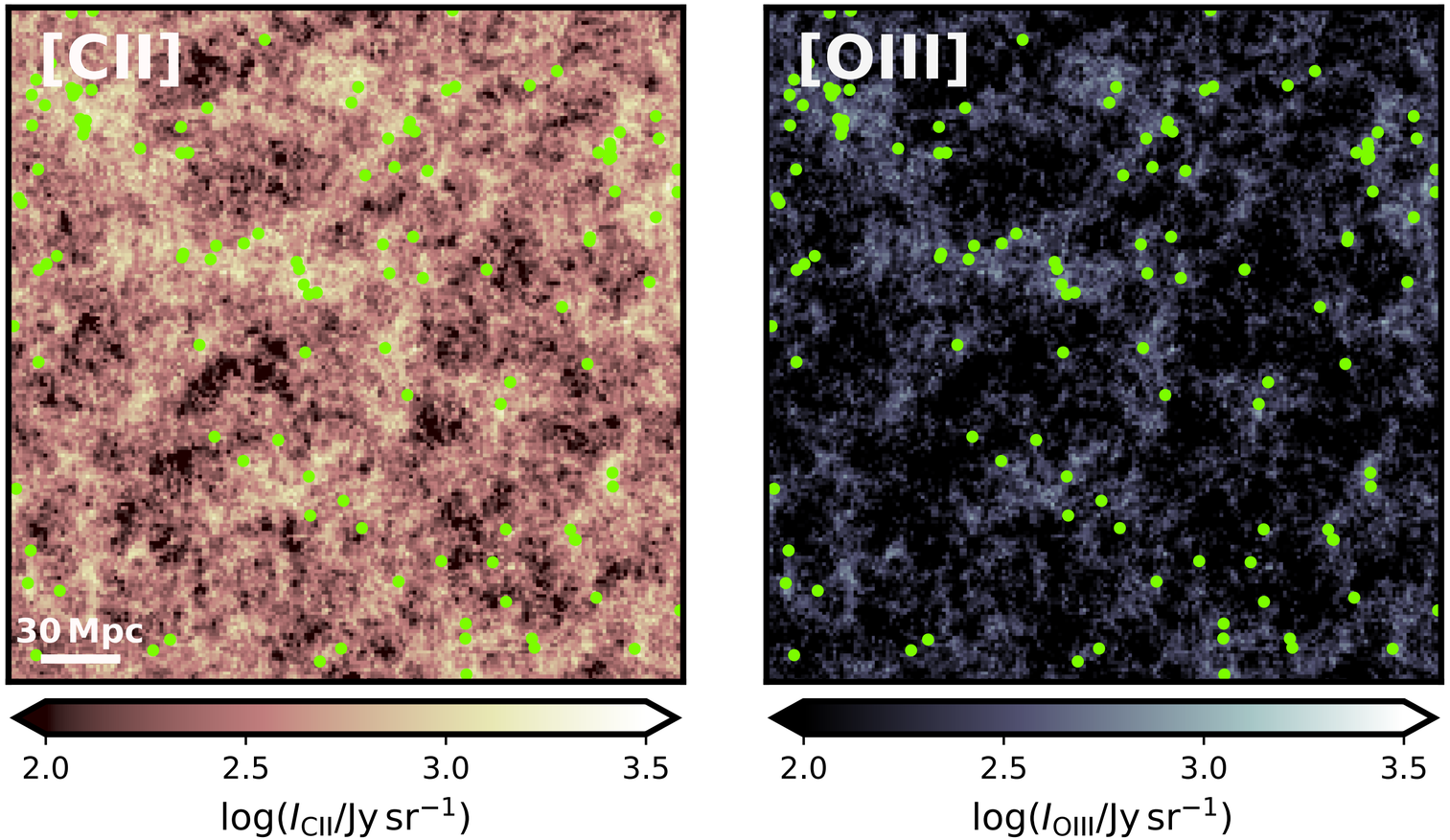

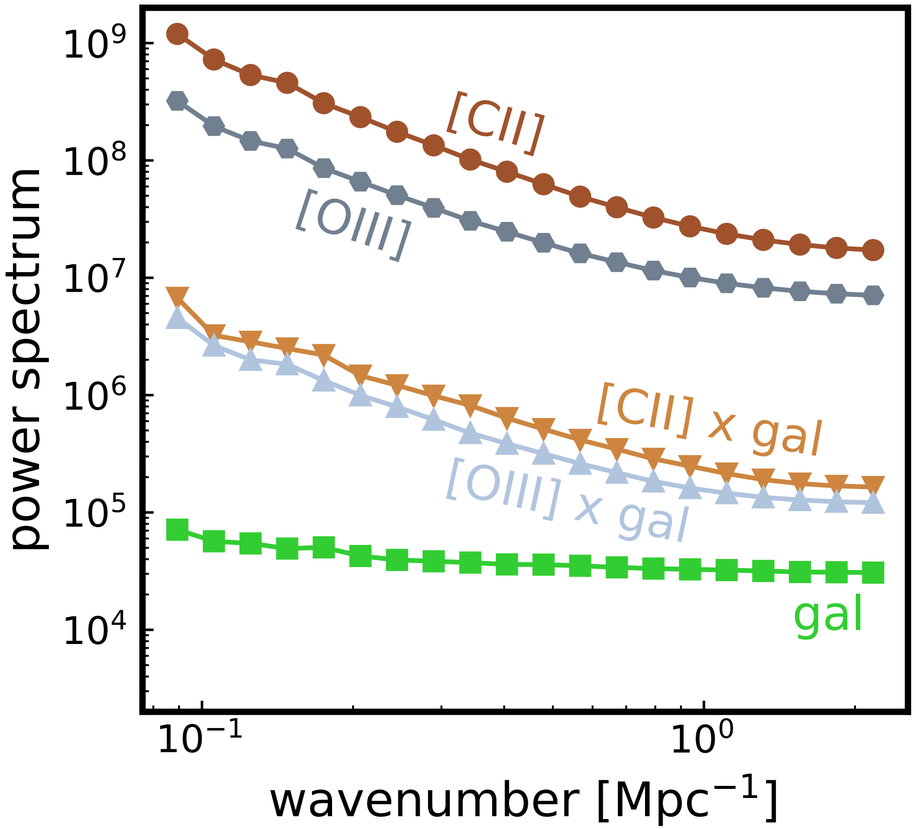

GS et al. (2025, in prep.)

Fisher matrix forecasts for [CII] & [OIII] joint analysis

Table 1. Instrument specifications of the LIM survey targeting $z \sim 6$ FIR emission lines

Target	$\Omega_{\rm survey}$ (deg^2)	$t_{\rm survey}$ (hr)	$N_{\rm pix}$	$\delta\nu$ (GHz)	$\Omega_{\rm beam}$ ($'^2$)	$V_{\rm vox}$ (Mpc^3)	$\sigma_{\rm N}$ (Jy s$^{1/2}$ sr^{-1})	$P_{\rm N}$ ((Jy/sr)^2 Mpc^3)
[C II]	4	4000	1000	3	0.6	17	5×10^5	2×10^8
[O III]	4	4000	1000	5	0.25	5	1×10^6	8×10^8

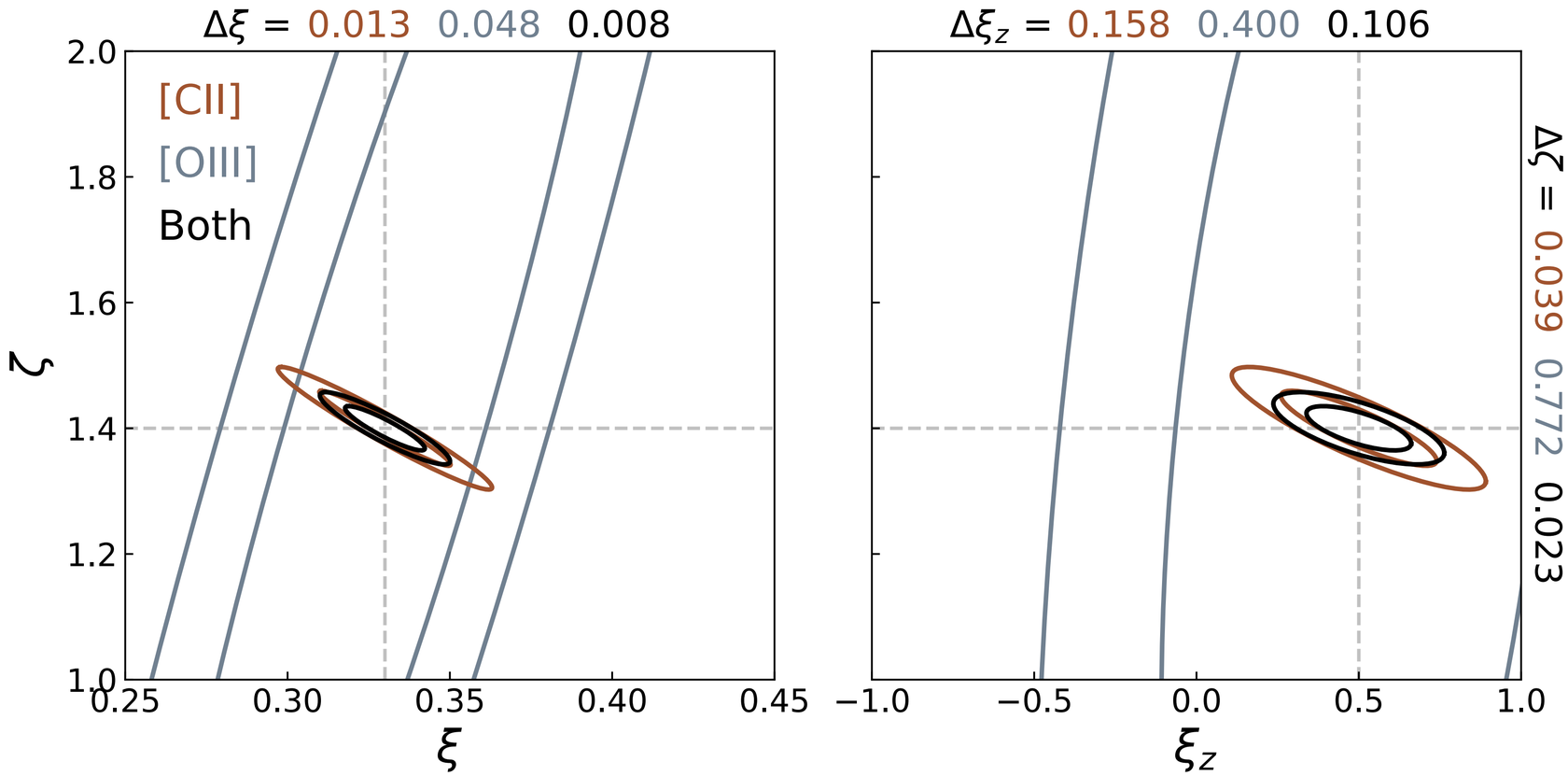

GS et al. (2025, in prep.)

Implicit likelihood inference (ILI) w/ LIMFAST-simulated PS

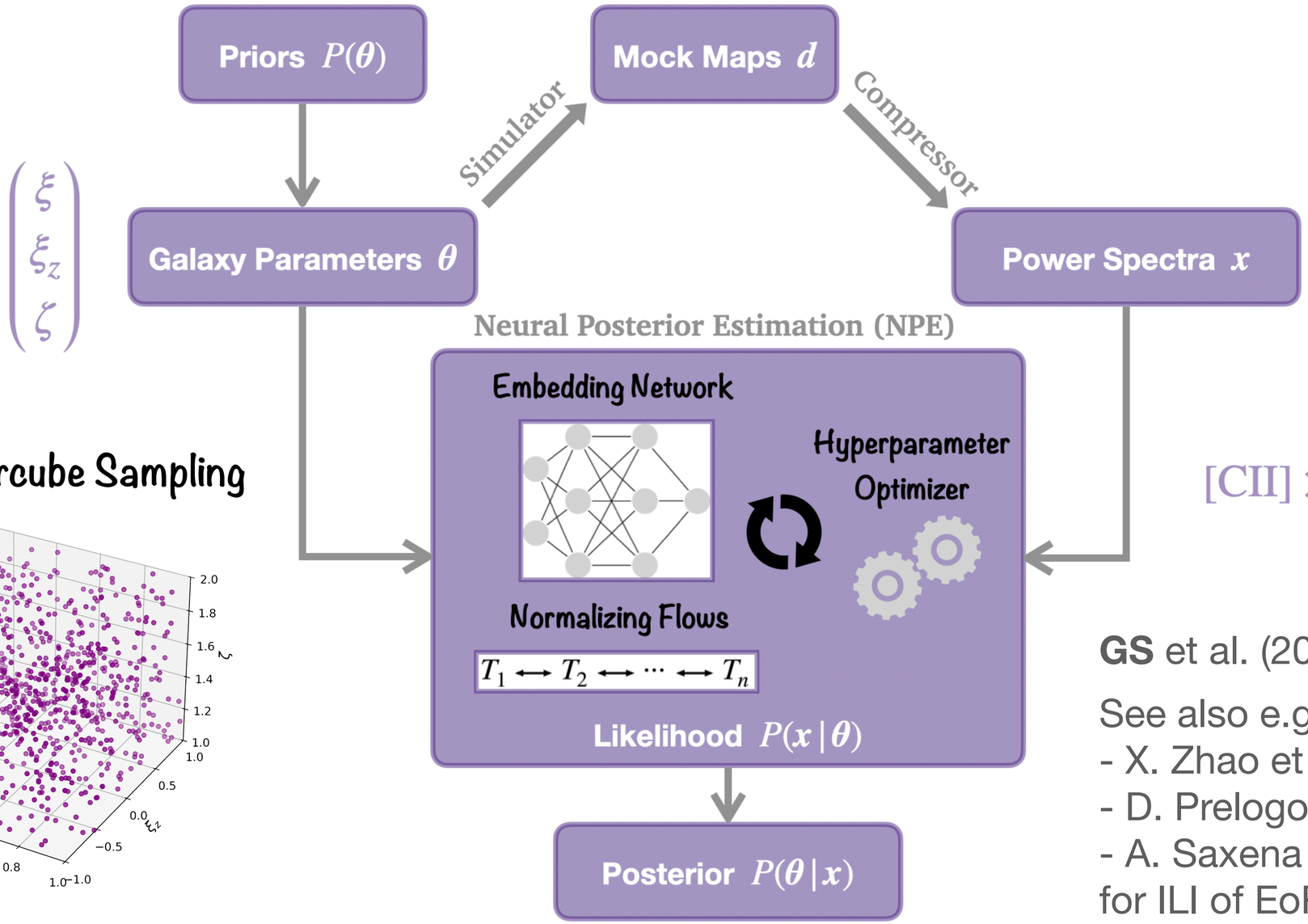

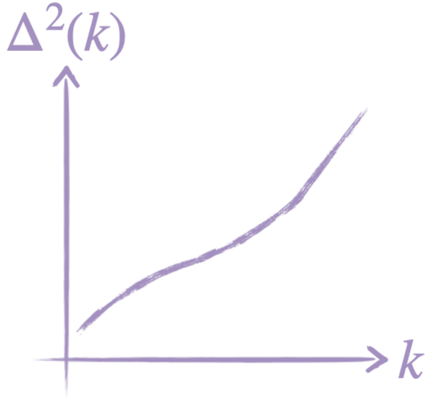

[CII], [OIII]

[CII] × LBGs, [OIII] × LBGs

Latin Hypercube Sampling

GS et al. (2025, in prep.)

See also e.g.,
- X. Zhao et al. (2022),
- D. Prelogović & A. Mesinger (2023)
- A. Saxena et al. (2023)

for ILI of EoR parameters from 21cm PS

Power spectra of [CII], [OIII], and cross-correlation w/ LBGs

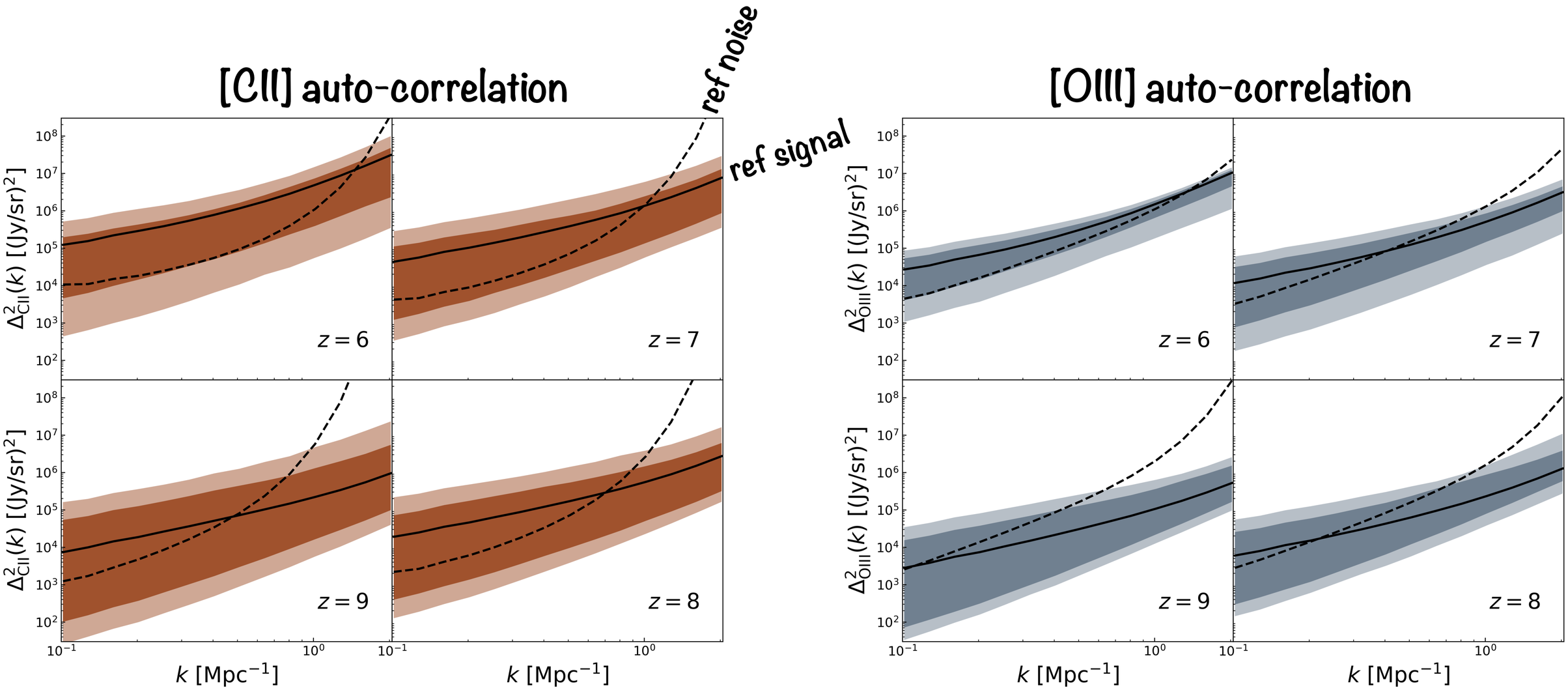

GS et al. (2025, in prep.)

Power spectra of [CII], [OIII], and cross-correlation w/ LBGs

[CII] x LBG cross-correlation

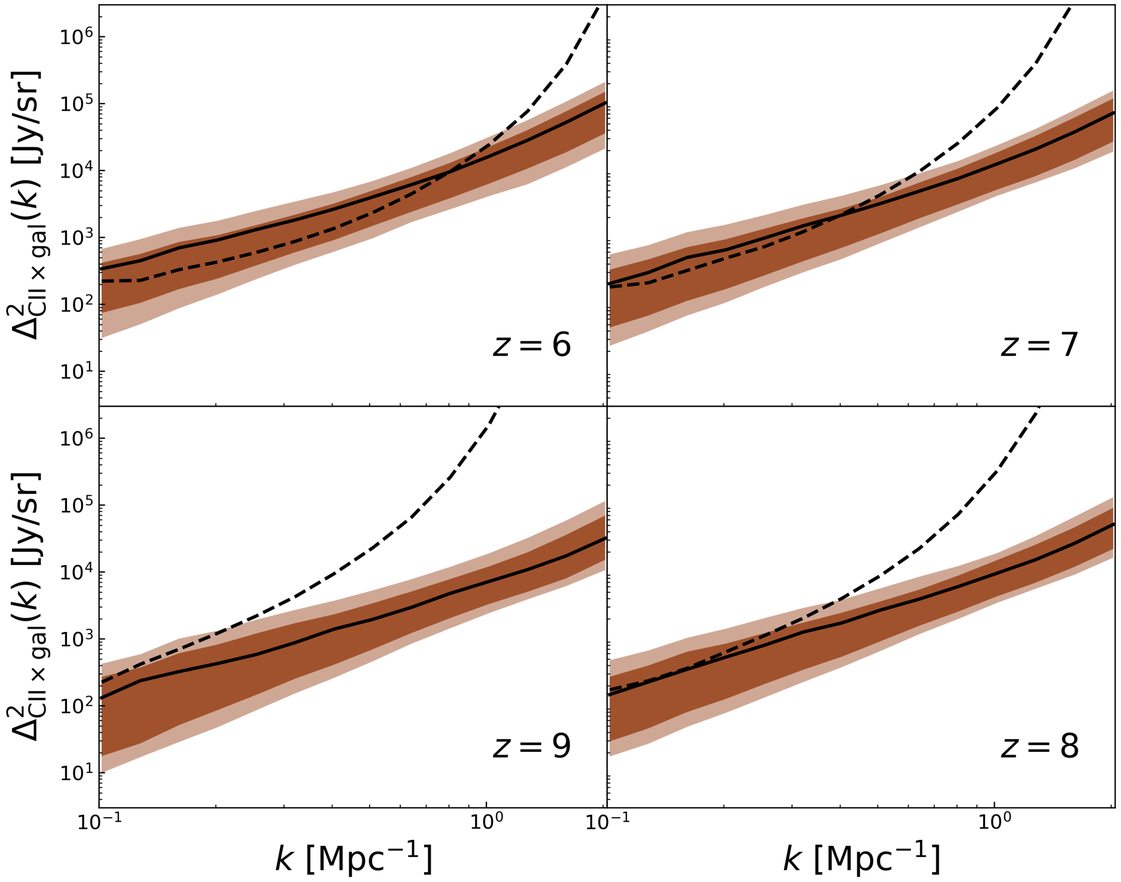

[OIII] x LBG auto-correlation

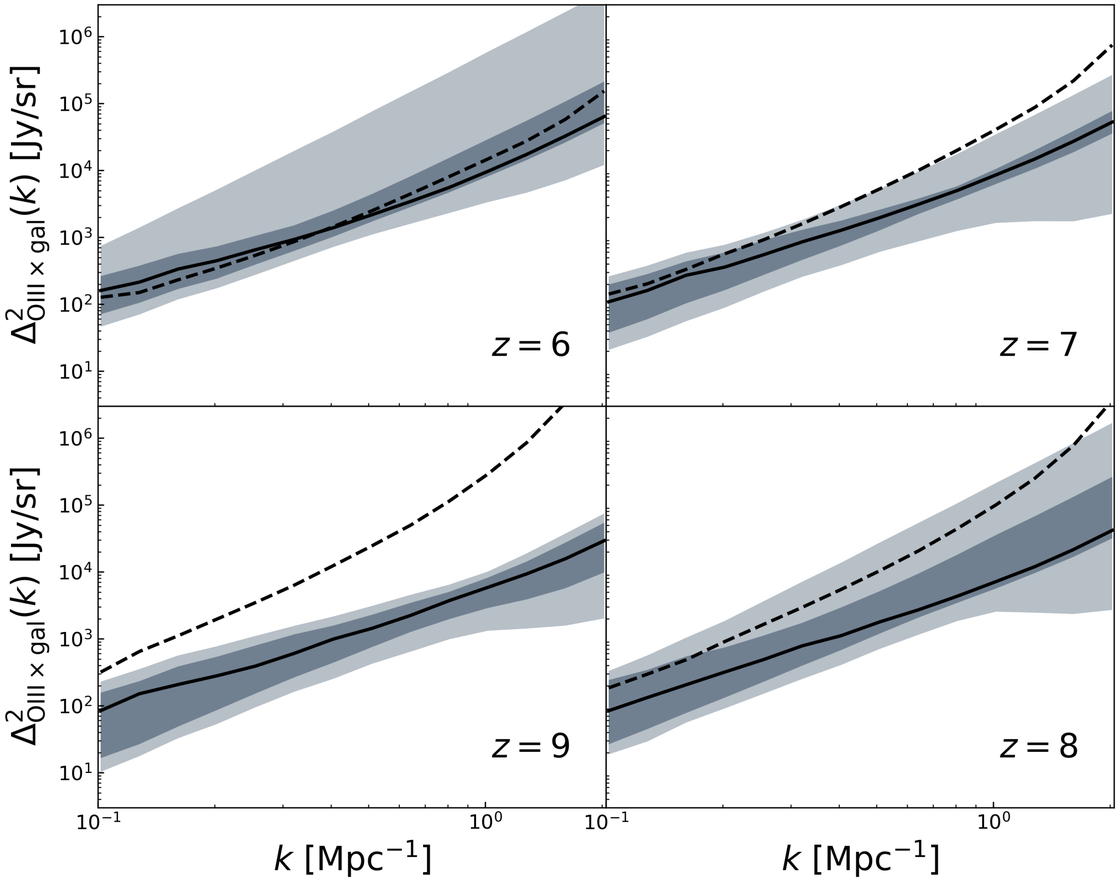

GS et al. (2025, in prep.)

Posterior from ILI w/ vs. w/o combining [CII] and [OIII]

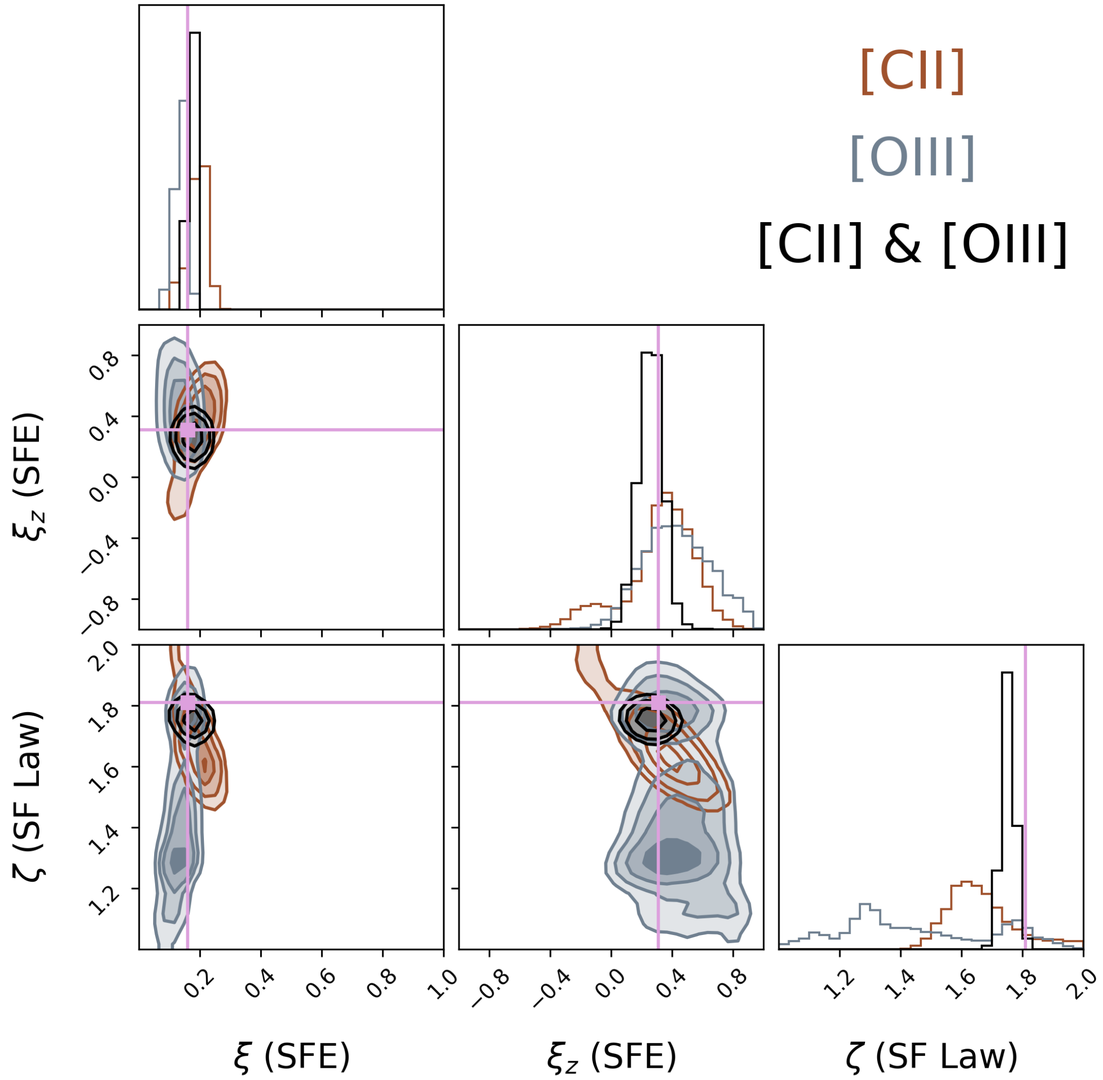

GS et al. (2025, in prep.)

- **Degeneracy reduced w/ [CII] & [OIII]**
- **Constraint on ζ greatly tightened**

Validating posterior predictiveness & coverage from ILI

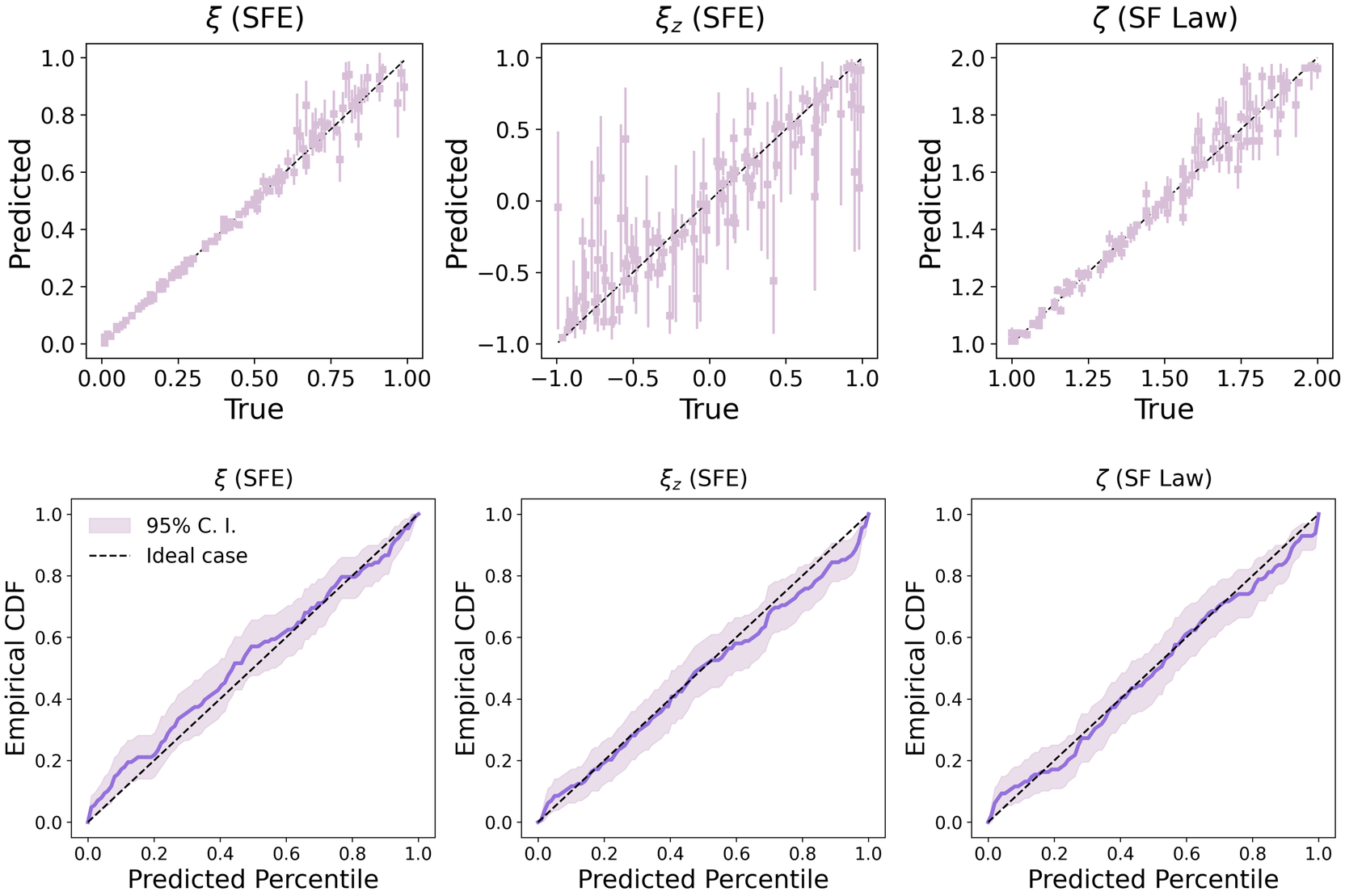

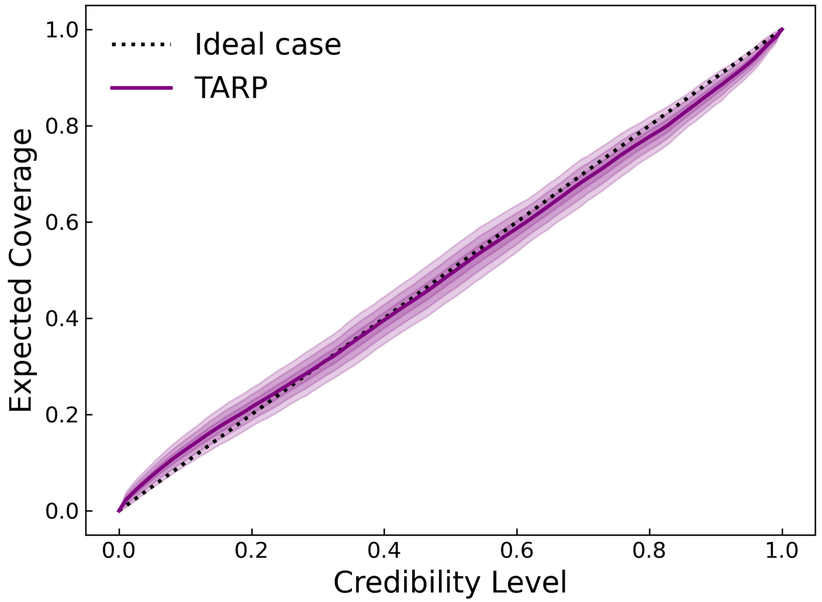

GS et al. (2025, in prep.)

Summary

- **Multi-tracer IM provides a powerful way to statistically and collectively study physical processes that govern the formation and evolution of early galaxies.**

- **As an example, combining [CII] and [OIII] LIM statistics (in foreseeable future) allows us to understand the SFE and SF law of high-redshift galaxies.**

- **Compared with traditional, explicit-likelihood methods, ILI enables more flexible and scalable analysis of galaxy formation physics using LIM summary statistics.**

BACK UP SLIDES